Physics in Medicine & Biology

IPEM Institute of Physics and Engineering in Medicine

PAPER

Monte Carlo calculation of beam quality correction factors in proton beams using TOPAS/GEANT4

Kilian-Simon Baumann[1,2], Sina Kaupa[2], Constantin Bach[2], Rita Engenhart-Cabillic[1,3] and Klemens Zink[1,2,3,4]

[1] Department of Radiotherapy and Radiooncology, University Medical Center Giessen-Marburg, Marburg, Germany
[2] Institute of Medical Physics and Radiation Protection, University of Applied Sciences, Giessen, Germany
[3] Marburg Ion-Beam Therapy Center (MIT), Marburg, Germany
[4] FIAS—Frankfurt Institute for Advanced Studies, Frankfurt, Germany

E-mail: kilian-simon.baumann@staff.uni-marburg.de

Keywords: proton dosimetry, proton therapy, beam quality correction factors, IAEA TRS-398 CoP, Monte Carlo, TOPAS, Geant4

Abstract

To provide Monte Carlo calculated beam quality correction factors (k_Q) for monoenergetic proton beams using TOPAS, a toolkit based on the Monte Carlo code GEANT4.

Monte Carlo simulations of six plane-parallel and four cylindrical ionization chambers were carried out. The latest ICRU 90 recommendations on key data for ionizing-radiation dosimetry were used to calculate the electronic stopping powers and to select the mean energy necessary to create an ion pair in air (W_{air}).

f_{Q_0} factors were calculated for a ^{60}Co spectrum at a depth of $5\,g\,cm^{-2}$. f_Q factors and f_Q/f_{Q_0} ratios as well as k_Q factors were calculated at the entrance region of monoenergetic proton beams with energies between 60 MeV and 250 MeV.

Additionally, perturbation correction factors for the Exradin A1SL ionization chamber at an energy of 250 MeV were calculated.

f_{Q_0} factors agreed within 0.7% or better, f_Q factors within 1.7% or better and f_Q/f_{Q_0} ratios within 2.2% or better with Monte Carlo calculated values provided in the literature. Furthermore, k_Q factors calculated in this work were found to agree within 1% or better with experimentally determined k_Q factors provided in the literature, with only two exceptions with deviations of 1.4% and 2.4%.

The total perturbation correction factor for the Exradin A1SL chamber was 0.969(7) and hence significantly different than unity in contrast to the assumption from the IAEA TRS-398 code of practice (CoP).

TOPAS/GEANT4 can be used to calculate k_Q factors in clinical proton beams. k_Q factors for six plane-parallel and four cylindrical ionization chambers were calculated and provided for the upcoming update of the IAEA TRS-398 CoP.

1. Introduction

The IAEA TRS-398 CoP for reference dosimetry in external radiotherapy beams (Andreo *et al* 2000) is currently being updated. The updated TRS-398 CoP will be based on the new ICRU 90 (Seltzer *et al* 2016) recommendations on key data for ionizing-radiation dosimetry. The RTNORM project (RTNORM 2019) is supporting the IAEA with fully Monte Carlo calculated k_Q factors for different ionization chambers and various radiotherapy beams that will be provided in the updated TRS-398 CoP. Furthermore, k_Q factors for monoenergetic proton beams will be provided which is not the case in the current TRS-398 CoP. Hence, there is a need for Monte Carlo calculated k_Q factors in monoenergetic proton beams. Please note that f_Q/f_{Q_0} ratios, which are the basis of Monte Carlo calculated k_Q factors, are the only part of k_Q factors that can be calculated using the Monte Carlo method. When using the term 'Monte Carlo calculated k_Q factors' we mean the Monte Carlo calculation of f_Q/f_{Q_0} ratios and subsequent derivation of k_Q factors by using the $W_{air,Q}$ values.

For ion beams the data of Monte Carlo calculated k_Q factors is scarce. Gomà *et al* (2016) used PENH (Salvat 2013) to calculate k_Q factors in monoenergetic proton beams for nine plane-parallel and three cylindrical ionization chambers. In the version of PENH that was used in that study no proton nuclear interactions were included and hence no secondary particles originating from non-elastic nuclear interactions were transported. Therefore, GAMOS (Arce *et al* 2014) a toolkit based on GEANT4 (Agostinelli *et al* 2003) was used to generate a phase space file in water directly in front of the ionization chamber while proton nuclear interactions were considered. This phase space file was subsequently used in PENH to calculate the dose absorbed in water in a reference volume and the dose absorbed in air in the sensitive volume of the ionization chambers. The so-calculated k_Q factors were compared to experimentally determined values from the literature and found to agree within 1%.

In a study by Gomà and Sterpin (2019) PENH was used to calculate k_Q factors in monoenergetic and modulated proton beams for nine plane-parallel and six cylindrical ionization chambers. In the version of PENH that was used in that study the simulation of proton nuclear interactions (and prompt-gamma emission) for all ICRU 63 (Barschall *et al* 2000) isotopes was included. The k_Q factors agreed with experimentally determined values on the 1% level. The f_Q factors calculated by Gomà and Sterpin (2019) were compared to f_Q factors calculated by Gomà *et al* (2016) for three chambers. Especially for high energies the results from both studies differed. Thus, the authors concluded that proton nuclear interactions should be included in the Monte Carlo calculation of k_Q factors, especially for high energies.

To the best of our knowledge, no other Monte Carlo code than PENH has been used for the calculation of k_Q factors in clinical proton beams so far. However, other Monte Carlo codes like TOPAS (Perl *et al* 2012) a toolkit based on GEANT4 as well as FLUKA (Ferrari *et al* 2005, Böhlen *et al* 2014) have been used for ionization chamber calculations in clinical proton beams: Wulff *et al* (2018) used TOPAS/GEANT4 to calculate f_Q factors for the IBA NACP-02 and Farmer NE 2571 ionization chamber in monoenergetic proton beams with energies between 70 MeV and 250 MeV. Two different nuclear interaction models were used and compared: binary cascade (BIC) and Bertini cascade (BERT). The f_Q factors calculated in that study agreed with those calculated by Gomà *et al* (2016) within 0.6% or better. The difference in f_Q factors for the different nuclear interaction models was 0.3% at maximum. Lourenço *et al* (2019) used FLUKA to calculate perturbation correction factors for three different PTW chambers. In the studies by Wulff *et al* (2018) and Lourenço *et al* (2019) only clinical proton beams and no photon beams (which are needed for the calculation of f_{Q_0} factors) have been investigated.

Hence, in a study by Baumann *et al* (2019) f_{Q_0} factors, f_Q factors and f_Q/f_{Q_0} ratios were calculated in a 1.25 MeV monoenergetic photon and a 150 MeV monoenergetic proton beam for simple air-filled cavities placed in a water phantom. The Monte Carlo codes PENH, FLUKA and TOPAS/GEANT4 were used. The resulting f_Q/f_{Q_0} ratios agreed within 0.7% or better between the codes. Since Gomà *et al* (2016) used PENH to calculate k_Q factors in monoenergetic proton beams in agreement with experimental data within 1%, the authors concluded that both FLUKA and TOPAS/GEANT4 can also be used for the calculation of k_Q factors in clinical proton beams. However, no k_Q factors for ionization chambers were calculated in that study.

Hence, the aim of this study is to calculate k_Q factors for six plane-parallel and four cylindrical ionization chambers in monoenergetic proton beams using the Monte Carlo code TOPAS/GEANT4. These k_Q factors shall be compared to experimentally determined k_Q factors provided in the literature. Furthermore, by providing k_Q factors calculated with a Monte Carlo code different than PENH we add important value, since for ion beams the data of Monte Carlo calculated k_Q factors is scarce and all Monte Carlo calculated k_Q factors for clinical proton beams provided in the literature have been derived using PENH.

Furthermore, the perturbation correction factor p_Q of ionization chambers is assumed to be 1 for proton beams in the IAEA TRS-398 CoP (Andreo *et al* 2000). Gomà and Sterpin (2019) calculated f_Q factors and water to air stopping power ratios $s_{w,air}$ in monoenergetic proton beams and hence were able to derive perturbation correction factors. The authors concluded that the perturbation correction factors of some ionization chambers might be significantly different than unity for proton beams. Hence, perturbation correction factors for one exemplary cylindrical ionization chamber shall be calculated in this study to clarify whether the assumption from the IAEA TRS-398 CoP is sufficiently accurate or not.

2. Materials and methods

2.1. Calculation of k_{Q,Q_0} factors

Monte Carlo k_{Q,Q_0} factors were calculated as (Andreo *et al* 2013):

$$k_{Q,Q_0} = \frac{f_Q}{f_{Q_0}} \frac{W_{air,Q}}{W_{air,Q_0}} = \frac{(D_w/\bar{D}_{air})_Q}{(D_w/\bar{D}_{air})_{Q_0}} \frac{W_{air,Q}}{W_{air,Q_0}} \tag{1}$$

Q denotes the user beam quality and Q_0 the reference beam quality. Note that, when ^{60}Co gamma radiation is the reference beam quality, the subscript Q_0 is typically omitted and k_Q is used instead of k_{Q,Q_0}. The factor f is both

chamber-specific and beam quality-dependent and gives the proportionality between the absorbed dose to water at the reference point when the chamber is absent (D_w) and the average absorbed dose to air in the cavity of the air-filled ionization chamber ($\bar{D}_{air}$) (Sempau *et al* 2004). $W_{air,Q}$ is the mean energy necessary to create an ion pair in air depending on the beam quality Q.

The dose values D_w and $\bar{D}_{air}$ were calculated using Monte Carlo simulations. The values for $W_{air,Q}$ were taken from the ICRU 90 (Seltzer *et al* 2016) (33.97 ± 0.12 eV for electrons, 34.44 ± 0.14 eV for protons).

2.2. Calculation of perturbation correction factors p_Q

Exemplary perturbation correction factors were calculated as described by Wulff *et al* (2008) for the cylindrical ionization chamber Exradin A1SL and a monoenergetic proton beam of 250 MeV. We calculated the following perturbation factors: p_{cel} that accounts for the central electrode in a cylindrical ionization chamber; p_{stem} that takes into account perturbations produced by the chamber stem; p_{wall} that considers that the material of the wall is different than water; the product of $p_{dis} \cdot p_{cav}$ that accounts for the effective point of measurement and the fact that the dose deposited in the cavity is an average dose deposited in a finite volume. From these perturbation correction factors we calculated the total perturbation correction factor p_Q as (Wulff *et al* 2008):

$$p_Q = p_{cel} \cdot p_{stem} \cdot p_{wall} \cdot p_{dis} \cdot p_{cav} \tag{2}$$

2.3. Possible influence of the death volume for ionization chambers

In a recent study by Pojtinger *et al* (2019) it was shown that the collecting volume of ionization chambers is not necessarily equal to the cavity of the ionization chamber. If a guard ring is present the resulting electric field lines can lead to a death volume in the vicinity of the guard ring inside the cavity. The resulting sensitive volume of the chamber is the cavity minus the death volume since charges produced in this death volume are not collected by the electrodes.

In this study we calculated the dose in the whole cavity of each chamber disregarding the potential death volume. Since the dose deposited in the sensitive volume might be different than the dose deposited in the complete cavity, this might have an effect on the calculated k_Q factors. In order to estimate the potential influence of this death volume on calculated k_Q factors, we calculated the dose deposited in the cavity of the Exradin A1SL chamber in a 250 MeV monoenergetic proton beam while the cavity was divided into 10 thin slabs (thickness of 0.4445 mm each). By investigating the space-resolved dose deposition we can derive the possible effect of the death volume.

2.4. Chamber geometries and materials

We investigated six plane-parallel ionization chambers (PTW Roos, PTW Markus, PTW Advanced Markus, IBA NACP-02, IBA PPC-05 and IBA PPC-40) and four cylindrical ionization chambers (NE 2571, PTW 30013, IBA FC65-G and Exradin A1SL). In table 1 the geometry and material compositions for the plane-parallel ionization chambers are summarized. For graphite the physical density ρ_g is shown since it varies between the manufacturers. The geometries of the cylindrical ionization chambers are too complex to be summarized in a table, hence, in figure 1 cross sections of the cylindrical ionization chambers are shown.

In table 2 all materials used in this study and their physical densities as well as the mean ionization potentials I used to calculate the electronic stopping powers are shown. For air and water we used the physical densities and I-values and for graphite the I-value as given in the ICRU 90.

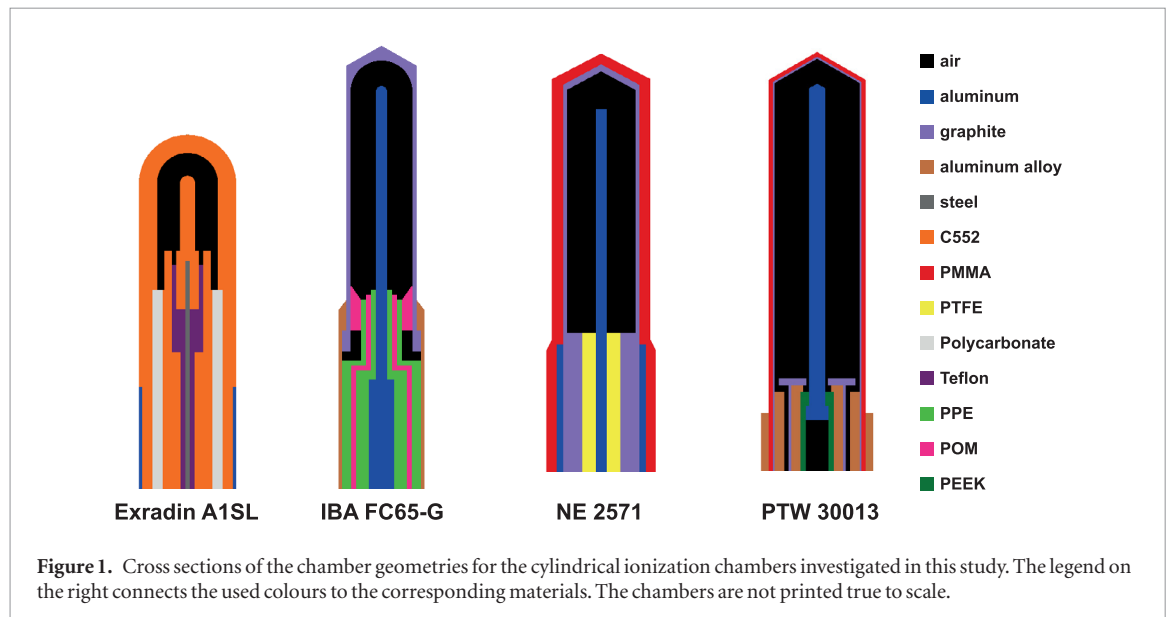### 2.5. Beam qualities and reference conditions

As reference beam quality Q_0 we used a ^{60}Co source. We used the energy spectrum as described by Mora *et al* (1999). The beam was uniform and parallel and impinging perpendicular on the water phantom surface. The field size was 10×10 cm^2. The beam was transported through vacuum between the source and the water phantom. Typically, a divergent source is used for high-energy photon simulations that develops a rectangular field at a certain depth in water at a certain distance to the source (see for instance (Wulff *et al* 2008, Zink and Wulff 2012, Gomà and Sterpin 2019)). However, such a source is not implemented in TOPAS/GEANT4 by default. Hence, we used an uniform and parallel beam.

As proton source we took an uniform and parallel beam of 10×10 cm^2 impinging perpendicular on the water phantom surface. We investigated eight different monoenergetic beams (60, 70, 80, 100, 150, 160, 200 and 250 MeV). The beam was transported through vacuum between the source and the water phantom.

For the simulations with the ^{60}Co spectrum we followed the IAEA TRS-398 CoP (Andreo *et al* 2000). That is, the reference depth z_{ref} was 5 g cm^{-2}. For the monoenergetic proton beams we used reference depths z_{ref} of 1 g cm^{-2} for low proton energies (60 and 70 MeV) and 2 g cm^{-2} for higher energies (E ⩾ 80 MeV). Beam quality correction factors k_Q for the cylindrical ionization chambers were only calculated for high energies (E ⩾ 150 MeV).

Table 1. Dimensions and materials of the plane-parallel chambers as investigated in this study. ρ_g denotes the physical density of the graphite used in each chamber.

Ionization chamber	Thickness of entrance window	Electrode spacing (mm)	Radius of sensitive volume (mm)	Thickness of collecting electrode
IBA				
NACP-02	0.1 mm PET 0.5 mm graphite $\left(\rho_g = 1.82 \text{ g cm}^{-3}\right)$	2	5	50 μm graphite $\left(\rho_g = 1.82 \text{ g cm}^{-3}\right)$ 0.25 mm PMMA
PPC-05	0.95 mm C552 50 μm graphite $\left(\rho_g = 1.82 \text{ g cm}^{-3}\right)$	0.6	5	50 μm graphite $\left(\rho_g = 1.82 \text{ g cm}^{-3}\right)$ 0.45 mm PPE
PPC-40	0.9 mm PMMA 0.1 mm graphite $\left(\rho_g = 0.93 \text{ g cm}^{-3}\right)$	2	8	0.1 mm graphite $\left(\rho_g = 0.93 \text{ g cm}^{-3}\right)$ 1 mm PMMA
PTW				
Advanced Markus	0.87 mm PMMA 0.3 mm PE	1	2.5	20 μm graphite $\left(\rho_g = 0.82 \text{ g cm}^{-3}\right)$
Markus	0.87 mm PMMA 0.4 mm Air 30 μm PE	2	2.65	20 μm graphite $\left(\rho_g = 1.72 \text{ g cm}^{-3}\right)$
Roos	1.1 mm PMMA 20 μm graphite $\left(\rho_g = 0.82 \text{ g cm}^{-3}\right)$	2	7.5	20 μm graphite $\left(\rho_g = 0.82 \text{ g cm}^{-3}\right)$

Figure 1. Cross sections of the chamber geometries for the cylindrical ionization chambers investigated in this study. The legend on the right connects the used colours to the corresponding materials. The chambers are not printed true to scale.

The absorbed dose to water D_w was calculated in a disc of 1 cm of radius and 250 μm of height. This disk was centered at z_{ref} in a water phantom of $20 \times 20 \times 20 \text{ cm}^3$ for the photon simulations and $20 \times 20 \times 5 \text{ cm}^3$ for the proton simulations. We chose to take a smaller water phantom for the proton simulations in order to reduce computing time and since proton backscatter can be considered negligible (Salvat 2013, Gomà *et al* 2016).

To calculate the average absorbed dose to air $\bar{D}_{air}$ in the cavity of the ionization chambers, each ionization chamber was positioned with its reference point at z_{ref}. For plane-parallel chambers, the reference point is at the center of the inner surface of the chamber's entrance window. For cylindrical chambers the reference point corresponds to the center of the cavity on the symmetry axis.

2.6. TOPAS/GEANT4

We used TOPAS (TOol for PArticle Simulation) version 3.1.p1 (Perl *et al* 2012), a toolkit based on the Monte Carlo code GEANT4 (GEometry And Tracking) version geant4-10-03-patch-01 (Agostinelli *et al* 2003). Since TOPAS is based on GEANT4, it uses the same physics models, processes, and interaction models. TOPAS

Table 2. Mass densities ρ and mean excitation energies I of the different materials as used in this study in alphabetical order.

Material	ρ (g cm^{-3})	I (eV)
Air	0.0012	85.7
Aluminum	2.70	166.0
Aluminum alloy	2.70	166.4
C552 (shonka)	1.76	86.8
Graphite	0.82–1.82	81.0
Polycarbonate	1.20	73.1
Polyether ether ketone (PEEK)	1.31	74.1
Polyether methacrylate (PMMA)	1.19	74.0
Polyethylene (PE)	0.93	56.5
Polyethylene terephthalate (PET)	1.50	78.7
Polyoxymethylene (POM)	1.43	77.4
Polyphenyl ether (PPE)	1.06	64.0
Polystyrene	1.05	68.7
Polytetrafluoroethylene (PTFE/Teflon)	2.25	99.1
Silicone	1.10	88.0
Steel	8.06	317.7
Water	0.9982	78.0

has been tested extensively against experimental data (Perl *et al* 2012, Testa *et al* 2013). TOPAS is capable of transporting various kinds of particles including photons, electrons, positrons, neutrons, protons, and heavy ions. In GEANT4, electro-magnetic (EM) interactions of the charged particles are grouped in the condensed history (CH) approach. A multiple scattering (MSC) algorithm is used to calculate the angular deflection of all soft collisions at the end of a given step. O'Brien *et al* (2016) and Wulff *et al* (2018) showed that TOPAS passes the Fano test within 0.1% for photons and 0.1%–0.2% for protons (depending on the beam geometry) as long as the appropriate physics lists are used and as long as these physics lists are tuned to calculate the radiation transport accurately enough. In another study by Simiele and DeWerd (2018) different transport parameters, multiple scattering algorithms and versions of GEANT4 were investigated with the conclusion that depending on the multiple scattering algorithm used, the step size has to be limited in order to pass the Fano test within less than 0.5%. Based on the findings by O'Brien *et al* (2016) and Wulff *et al* (2018), Baumann *et al* (2019) showed that TOPAS/GEANT4 can be used to calculate f_Q/f_{Q_0} ratios (which are the basis of Monte Carlo calculated k_Q factors, compare equation (1)) in clinical proton beams for simple air-filled cavities placed in a water phantom. Hence, in this study we used the same physics lists and settings as used by Baumann *et al* (2019). For the photon simulations we used the physics list **g4em-standard_opt3** that makes use of the *G4UrbanMscModel* (Urban 2002) to describe the multiple scattering of all charged particles. For the proton simulations we used the physics list **g4em-standard_opt4** which makes use of the models *WentzelVI* (Ivanchenko *et al* 2010) and *Goudsmit–Saunderson* (Goudsmit and Saunderson 1940a, 1940b) for the multiple scattering of charged particles: for electrons and positrons with energies below 100 MeV, the *Goudsmit–Saunderson* model is used. For electrons and positrons with an energy above 100 MeV and for protons with energies below 500 MeV, the *WentzelVI* model is used. The multiple scattering models used in this study are summarized in table 3. Please note that the Goudsmit–Saunderson model is not implemented by default in the version geant4-10-03-patch-01 which is used in this study but has been implemented by us.

We used the physics list **g4h-phy_QGSP_BIC_HP** to manage the simulation of non-elastic nuclear interactions. The *Binary Cascade* model (Folger *et al* 2004) is used in this list for inelastic nucleon-nucleus processes. Furthermore, we used the default physics lists **g4ion-binarycascade**, **g4decay**, **g4h-elastic_HP** and **g4stopping**.

To control the length of a step in the CH, the parameter *dRoverR* is used in GEANT4. This parameter describes the maximum length of a step in relation to the residual range of the particle. For the photon simulations we set *dRoverR* to 0.003, for the proton simulation to 0.05. While losing energy, the maximum length of a step in the CH decreases until it gets smaller than the *finalRange*, below which the particle is ranged out in a single step. For the photon simulations we set *finalRange* to 1 nm, for the proton simulations to 100 nm. The parameter controlling the production of secondaries is given in units of length in GEANT4. Secondary particles with a *continuous slowing down approximation* range (R_{CSDA}) lower than this production cut are absorbed on the spot. The default production cut in the whole geometry was set to 500 μm, corresponding to $\sim$200 keV electrons in water. Within the ionization chamber and a surrounding envelope, the production cut was set to 1 μm (corresponding to <10 keV electrons in water). Note that in the study by Baumann *et al* (2019) a production cut of 0.065 μm was used (which corresponds to $\sim$1 keV electrons in water). In order to save computing time, we increased this value. We checked that this larger production cut has no significant influence on the calculation of f_{Q_0} and f_Q factors. This

Table 3. Multiple scattering models used in TOPAS/GEANT4 for the photon and proton simulations.

Radiation field	Multiple scattering model for e^+/e^-	Multiple scattering model for primaries
^{60}Co spectrum	Urban model	/
Monoenergetic protons	Goudsmit–Saunderson (E $\leqslant$ 100 MeV)	Wentzel VI (E $\leqslant$ 500 MeV)
	Wentzel VI (E $>$ 100 MeV)	

Table 4. Production cuts and transport simulation parameters used in TOPAS/GEANT4 for the photon and proton simulations.

Region	Production cut (μm)	*dRoverR*		*finalRange* (nm)	
		Photon-sim.	Proton-sim.	Photon-sim.	Proton-sim.
Scoring volume and envelope	1	0.003	0.05	1	100
Water phantom	500	0.003	0.05	1	100

has also been investigated for f_Q factors in proton beams by Wulff *et al* (2018) with the same result. To ensure that the secondary particle fluence in the ionization chamber is not affected by the higher production cut in the water phantom, we used an envelope surrounding the ionization chamber with a thickness equal to the production cut applied in the water phantom (500 μm) multiplied by a safety factor of 1.2. The safety factor of 1.2 is applied to account for the possibility that an electron may travel a distance larger than R_{CSDA} due to energy-loss straggling (Sempau and Andreo 2006). Since the lowest energy GEANT4 can handle is 990 eV by default, the production cut is automatically adapted in materials where the production cut of 1 μm corresponds to an energy $<$990 eV. For example, the production cut in air is set to 47.2 μm, which is the maximum range of 990 eV electrons in air. All production cuts and transport simulation parameters are summarized in table 4.

No variance reduction techniques were used. The statistical uncertainties were estimated by combining the uncertainties from independent runs performed with different random seeds as described in Bielajew (2016).

3. Results and discussion

3.1. f_{Q_0} factors for the ^{60}Co spectrum

In table 5 the Monte Carlo calculated f_{Q_0} factors for the ^{60}Co spectrum for all ionization chambers investigated in this study are shown. The values within parenthesis correspond to one standard uncertainty in the last digit. Furthermore, combined data for $f_{Q_0} = (s_{\text{w,air}})_{Q_0} \cdot p_{Q_0}$ as provided by the upcoming revision of the TRS-398 CoP (Andreo *et al* 2019) is shown. The given values are the average of 16 different f_{Q_0} factors all calculated with Monte Carlo codes (EGS*nrc*, PENH, PENELOPE, and TOPAS/GEANT4, while the TOPAS/GEANT4 results are those from this study). Chambers were modeled using blue prints or geometries published in former studies.
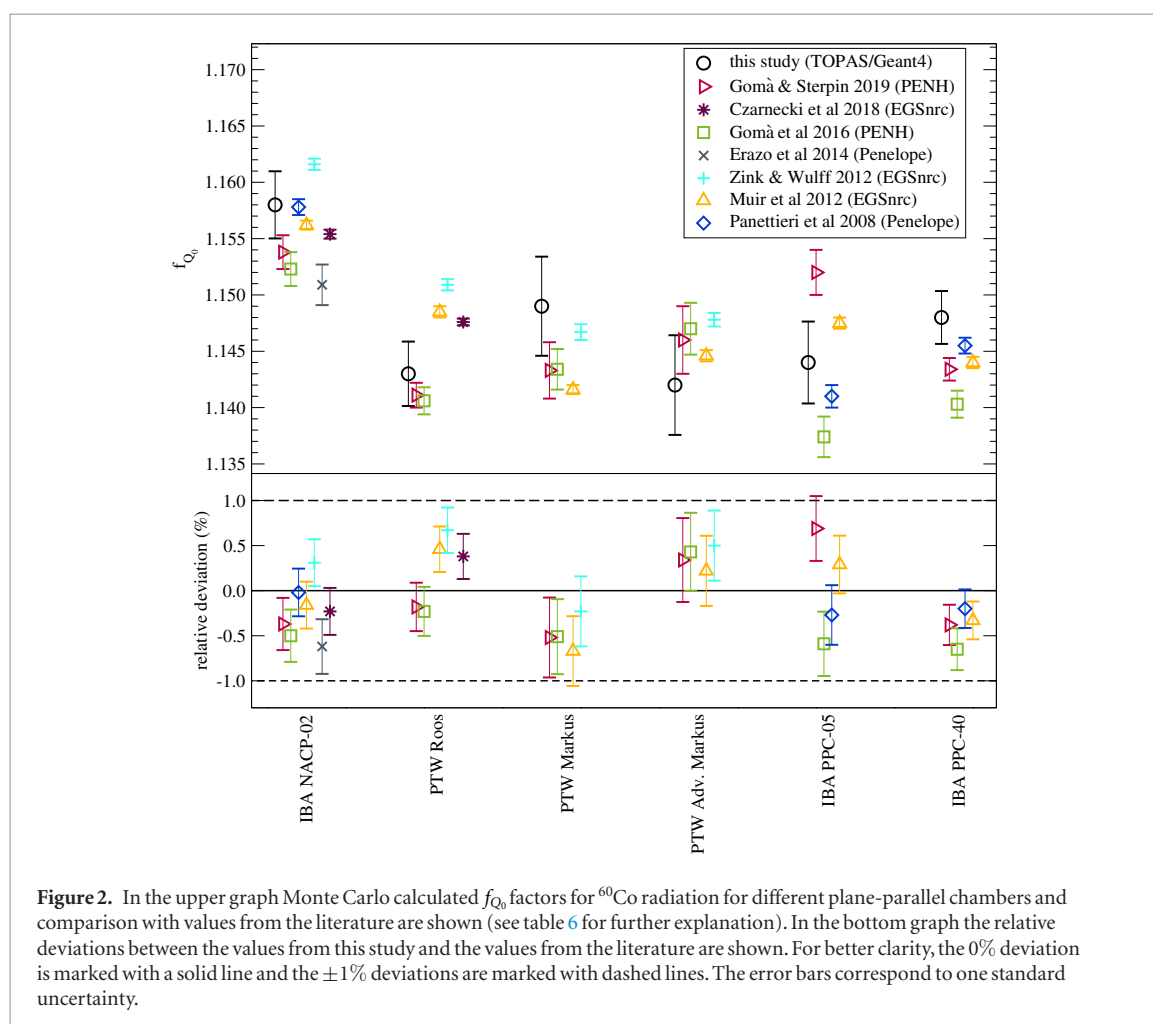
For all chambers the f_{Q_0} factors calculated in this study agree within one standard uncertainty with the values provided by Andreo *et al* (2019).

In figures 2 and 3 in the upper panels the f_{Q_0} factors for the plane-parallel and cylindrical ionization chambers are shown along with various values published in the literature. In the bottom panel the relative deviations between the values from this study and the values from the literature are shown. The values published in the literature were derived using different Monte Carlo codes and partly different sets of *I*-values. An overview of these characteristics is given in table 6.

For each chamber the deviation between the f_{Q_0} factor calculated in this study using TOPAS/GEANT4 and the factors published in the literature is smaller than 0.7% (independently on the choice of *I*-values). For almost each chamber the f_{Q_0} factor calculated in this study agrees with each published value within two standard deviations or better. The only exceptions are for the PTW Roos chamber and the results from Zink and Wulff (2012) as well as the IBA PPC-40 chamber and the results from Gomà *et al* (2016). Taking into account the variance between the f_{Q_0} factors published in the literature using different Monte Carlo codes and sets of *I*-values, TOPAS/GEANT4 can be used equivalently for the calculation of f_{Q_0} factors for both plane-parallel and cylindrical ionization chambers in ^{60}Co beams as long as the physics settings are adapted accordingly. Note that the variance between f_{Q_0} factors published in the literature is larger for plane-parallel ionization chambers compared to cylindrical chambers.

Table 5. Monte Carlo calculated f_{Q_0} factors for ^{60}Co radiation for different plane-parallel and cylindrical ionization chambers. The values within parenthesis correspond to one standard uncertainty in the last digit.

Chamber	f_{Q_0} this study	f_{Q_0} Andreo *et al* (2019)
PTW Roos	1.143(3)	1.142(5)
PTW Markus	1.149(4)	1.143(5)
PTW Adv. Markus	1.142(4)	1.143(5)
IBA NACP-02	1.158(3)	1.154(5)
IBA PPC-05	1.144(4)	1.141(5)
IBA PPC-40	1.148(2)	1.142(5)
NE 2571	1.110(3)	1.108(4)
PTW 30013	1.112(3)	1.109(4)
IBA FC65-G	1.111(3)	1.108(4)
Exradin A1SL	1.102(5)	1.103(4)

Figure 2. In the upper graph Monte Carlo calculated f_{Q_0} factors for ^{60}Co radiation for different plane-parallel chambers and comparison with values from the literature are shown (see table 6 for further explanation). In the bottom graph the relative deviations between the values from this study and the values from the literature are shown. For better clarity, the 0% deviation is marked with a solid line and the ±1% deviations are marked with dashed lines. The error bars correspond to one standard uncertainty.
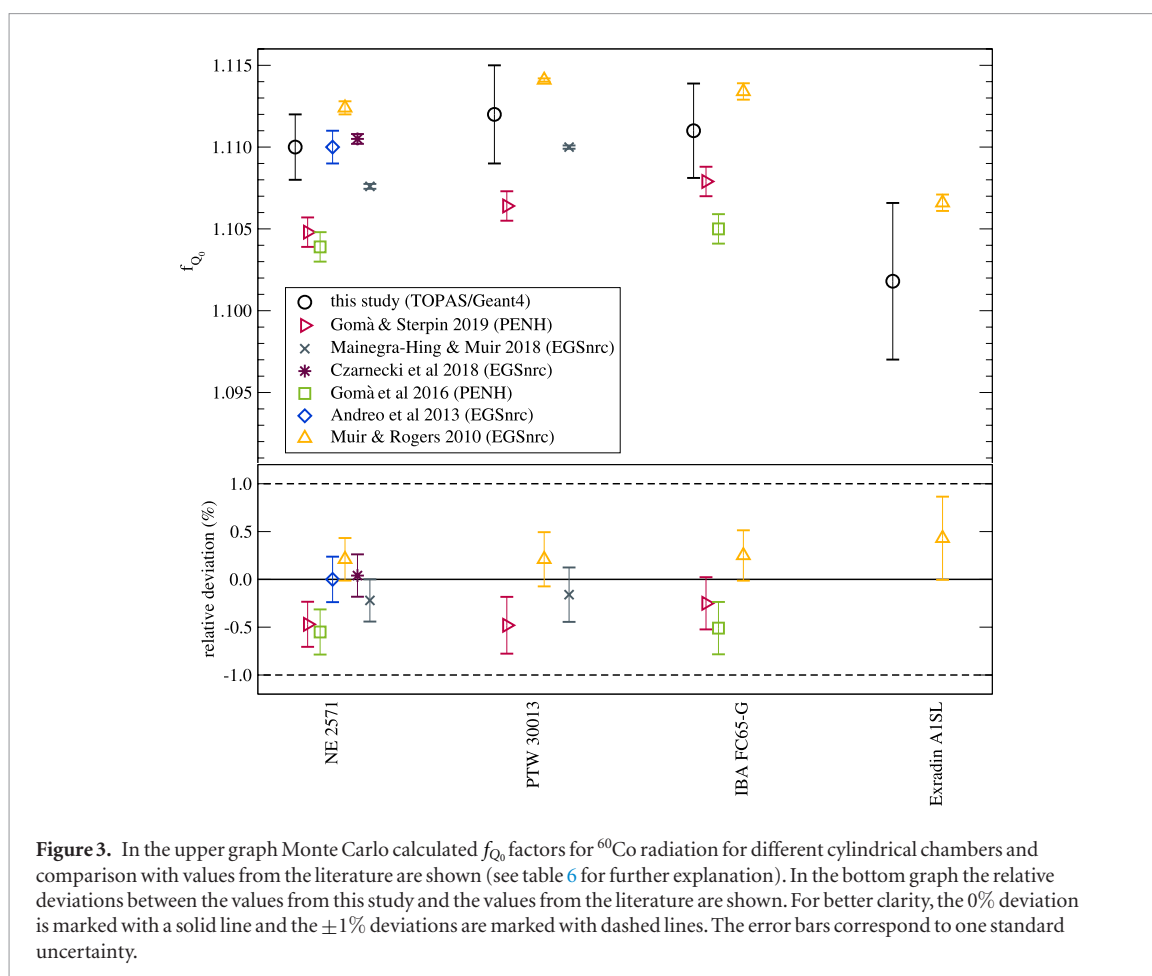
3.2. f_Q factors for monoenergetic proton beams

In table 7 the f_Q factors for all ionization chambers investigated in this study are shown as a function of the initial energy of the monoenergetic proton beams. The depth z_{ref} at which the chambers were positioned is depicted as well. The values within parenthesis correspond to one standard uncertainty in the last digit(s).

Furthermore, the water to air stopping power ratios $s_{w,air}$ as calculated by Gomà and Sterpin (2019) are given for the different beam qualities in order to estimate perturbation correction factors as done in section 3.3.

Figures 4 and 5 show the f_Q factors from this study along with f_Q factors published in the literature. Some of the values published in the literature were derived using different Monte Carlo codes. An overview of the corresponding characteristics is given in table 8.

For the IBA NACP-02 the f_Q factors agree within one standard deviation for energies up to 150 MeV. For higher energies the differences are up to 1.2% between this study and Gomà and Sterpin (2019), 0.9% between

Figure 3. In the upper graph Monte Carlo calculated f_{Q_0} factors for ^{60}Co radiation for different cylindrical chambers and comparison with values from the literature are shown (see table 6 for further explanation). In the bottom graph the relative deviations between the values from this study and the values from the literature are shown. For better clarity, the 0% deviation is marked with a solid line and the $\pm 1\%$ deviations are marked with dashed lines. The error bars correspond to one standard uncertainty.

this study and Gomà *et al* (2016) and 0.5% between this study and Wulff *et al* (2018). The reason for the difference in f_Q factors between this study and Wulff *et al* (2018) is that in this study the geometry of the IBA NACP-02 is slightly different and a smaller value for *dRoverR* and *finalRange* has been taken.

For the PTW Roos chamber the differences between the f_Q factors calculated in this study and the values from Gomà and Sterpin (2019) are significant for both low and high energies. The maximum deviation is -1% for an energy of 250 MeV while the deviation for low energies is about 0.4%. Differences between the f_Q factors calculated in this study and the values from Lourenço *et al* (2019) are $\sim$0.1% for the energies 60 MeV and 250 MeV while the deviation for an energy of 150 MeV is 0.4%.

For all plane-parallel chambers it can be seen that the f_Q factors agree within two standard uncertainties or better between this study and the studies by Gomà and Sterpin (2019) and Gomà *et al* (2016) for low energies and begin to diverge for higher energies. Only for the PTW Roos chamber as already mentioned and the PTW Adv. Markus chamber significant differences in the f_Q factors between the studies can be seen for low energies. Note that Gomà *et al* (2016) used a different geometry for the IBA PPC-05 chamber, hence the deviations of the f_Q factors relative to this study are quite large. The largest deviation of f_Q factors between this study and the values published in the literature is 1.7% and can be seen for the PTW Markus chamber at an energy of 250 MeV.

For the f_Q factors for cylindrical ionization chambers as shown in figure 5 the factors calculated in this study agree within $<$0.1% with those calculated by Wulff *et al* (2018) for 150 MeV and 200 MeV. For 250 MeV a deviation of $\sim$0.5% is visible. In contrast to the calculation of the IBA NACP-02 chamber, the geometry of the NE 2571 chamber used in this study is exactly the same as used by Wulff *et al* (2018). The only remaining difference between these two studies is that in this study a smaller value for *dRoverR* and *finalRange* has been taken.

For all cylindrical chambers the f_Q factors calculated in this study agree within one standard uncertainty with the factors calculated by Gomà *et al* (2016). Again, the values calculated by Gomà and Sterpin (2019) agree with the factors from this study only for low energies (e.g. 150 MeV) within one standard uncertainty. For higher energies the values do not agree within two standard uncertainties. The largest deviation of 1.3% can be seen for the NE 2571 chamber at an energy of 250 MeV.

In general, the agreement between the values from this study and the values from Gomà *et al* (2016) is better than the agreement between this study and the values from Gomà and Sterpin (2019). The difference between these two studies (Gomà and Sterpin (2019) and Gomà *et al* (2016)) is that in the study from 2019 proton nuclear

9

Table 6. Description of the values for f_{Q_0} from the literature in chronological order.

Study	Monte Carlo code	I_w (eV)	I_g (eV)	Comments
Gomà and Sterpin (2019)	PENH	78	81.1	—
Czarnecki et al (2018)	EGS*nrc*	78	81.1	Values provided in private communication
Mainegra-Hing and Muir (2018)	EGS*nrc*	78	81.1	Values provided in Gomà and Sterpin (2019)
Gomà et al (2016)	PENH	78	81.1	—
Erazo et al (2014)	PENELOPE-2011	75	78	Values provided in Gomà et al (2016)
Andreo et al (2013)	EGS*nrc*	78	81.1	—
Zink and Wulff (2012)	EGS*nrc*	75	78	Calculated perturbation correction factors p_{Q_0}: $f_{Q_0} = p_{Q_0} \cdot s_{w,air}$ ($s_{w,air} = 1.133$)
Muir et al (2012)	EGS*nrc*	75	78	Values provided in Gomà et al (2016)
Muir and Rogers (2010)	EGS*nrc*	75	78	Values provided in private communication
Panettieri et al (2008)	PENELOPE-2006	75	78	Used three different ^{60}Co sources: we used the weighted mean of the corresponding f_{Q_0} factors

Table 7. Monte Carlo calculated f_Q factors for monoenergetic proton beams as a function of initial proton energy and the depth z_{ref} at which the chambers were positioned. The values within parenthesis correspond to one standard uncertainty in the last digit(s).

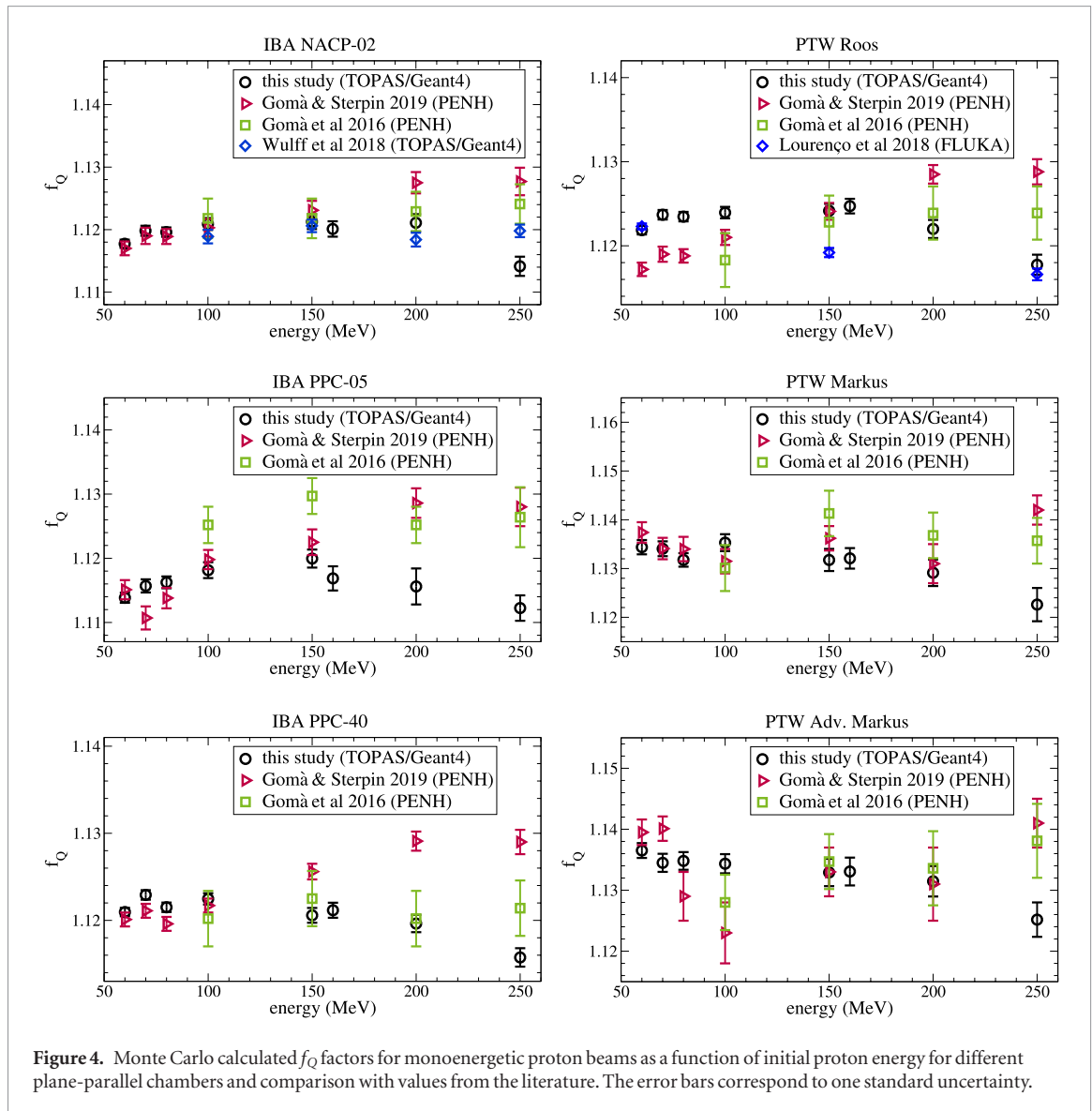| Q	60 MeV	70 MeV	80 MeV	100 MeV	150 MeV	160 MeV	200 MeV	250 MeV
z_{ref} (g cm^{-2})	1	1	2	2	2	2	2	2
$s_{w,air}$	1.130	1.130	1.130	1.130	1.129	1.129	1.129	1.129
PTW Roos	1.1219(5)	1.1237(6)	1.1235(6)	1.1239(7)	1.1242(8)	1.1247(9)	1.1220(11)	1.1177(12)
PTW Markus	1.1344(15)	1.1341(15)	1.1318(14)	1.1353(17)	1.1318(23)	1.1321(21)	1.1291(27)	1.1226(34)
PTW Adv. Markus	1.1365(12)	1.1345(15)	1.1348(15)	1.1343(16)	1.1329(22)	1.1331(23)	1.1315(25)	1.1252(28)
IBA NACP-02	1.1177(7)	1.1198(8)	1.1196(7)	1.1209(10)	1.1213(12)	1.1201(12)	1.1211(14)	1.1141(15)
IBA PPC-05	1.1139(8)	1.1157(10)	1.1162(9)	1.1181(12)	1.1200(14)	1.1169(19)	1.1156(28)	1.1122(20)
IBA PPC-40	1.1210(5)	1.1229(5)	1.1215(5)	1.1225(6)	1.1206(8)	1.1212(9)	1.1196(10)	1.1157(11)
NE 2571					1.1232(9)	1.1225(9)	1.1185(11)	1.1115(12)
PTW 30013					1.1257(9)	1.1244(9)	1.1211(11)	1.1168(11)
IBA FC65-G					1.1237(10)	1.1223(10)	1.1192(11)	1.1137(12)
Exradin A1SL					1.1073(23)	1.1036(26)	1.1035(30)	1.0938(34)

Table 8. Description of the values for f_Q from the literature in chronological order.

Study	Monte Carlo code	I_w (eV)	I_g (eV)	Comments
Gomà and Sterpin (2019)	PENH	78	81.1	Chamber positioned at same depths as in this study
Lourenço *et al* (2019)	FLUKA	78	81.1	Calculated perturbation correction factors and stopping power ratios Values provided in private communication Used a slightly different ($\sim$180 μm) depth No transport of electrons
Wulff *et al* (2018)	TOPAS/GEANT4	78	81.1	We used the values derived using the BIC model Values for 70 MeV not considered since a different depth has been used
Gomà *et al* (2016)	PENH	78	81.1	Values for 70 MeV not considered since a different depth has been used

interactions have been activated in PENH. In the study from 2016 no proton nuclear interactions have been included in PENH. However, the simulations were combined with simulations performed with GAMOS (Arce *et al* 2014) a toolkit based on GEANT4 where nuclear interactions were included, which might explain the better agreement between this study and the study by Gomà *et al* (2016). Furthermore, Gomà and Sterpin (2019) discussed that the differences in f_Q factors for higher energies might be due to differences in the nuclear interaction models. To investigate this statement, we recalculated the f_Q values for the IBA NACP-02 and NE 2571 for an energy of 250 MeV without the use of nuclear interaction models (n.i.m.) by deactivating the physics list **g4h-phy_QGSP_BIC_HP**. The results are shown in figure 6: PENH with n.i.m. corresponds to the values from Gomà and Sterpin (2019) while PENH with n.i.m. from GEANT4 corresponds to the values from Gomà *et al* (2016). The f_Q factors calculated with TOPAS/GEANT4 increase by roughly 1.5% when deactivating the nuclear interaction model. For PENH it is the other way round: the f_Q factors are larger when nuclear interaction models are activated. Interestingly, the values calculated with TOPAS/GEANT4 without the activation of nuclear interaction models agree with those calculated with PENH when these models are activated. However, it is not possible to identify the role of nuclear interaction models for the calculation of f_Q factors in proton beams from these results. This remains an issue to be solved in further investigations.

3.3. Perturbation correction factors for monoenergetic proton beams

From the f_Q factors and water to air stopping power ratios $s_{w,air}$ as shown in table 7 the total perturbation correction factors p_Q can be derived as $p_Q = f_Q/(s_{w,air})_Q$. It can be seen that for some chambers and energies the perturbation correction factors are significantly different than unity in contrast to the assumption from the IAEA TRS-398 CoP (Andreo *et al* 2000). To investigate which part of the chamber might lead to this difference we calculated the perturbation correction factors for the Exradin A1SL chamber at 250 MeV. The results are shown in table 9. The perturbation factor with the largest influence is p_{wall} which accounts for the influence of the chamber wall. The total perturbation correction factor p_Q is 0.969(7). Hence, it can be concluded that the assumption of the IAEA TRS-398 CoP (that all perturbation correction factors in proton beams are 1 for all

Figure 4. Monte Carlo calculated f_Q factors for monoenergetic proton beams as a function of initial proton energy for different plane-parallel chambers and comparison with values from the literature. The error bars correspond to one standard uncertainty.

ionization chambers) might not be sufficiently accurate for all chambers and proton energies—especially in the case for the factor p_{wall}.

3.4. k_Q factors for monoenergetic proton beams

In table 10 the k_Q factors for all ionization chambers investigated in this study are shown as a function of the initial energy of the monoenergetic proton beams. The depth z_{ref} at which the chambers were positioned is depicted as well. The values within parenthesis correspond to one standard uncertainty in the last digit(s).

To compare the results from this study with Monte Carlo calculated values published in the literature, we decided not to compare the k_Q factors itself but the f_Q/f_{Q_0} ratios which are the basis of Monte Carlo calculated k_Q factors. In figures 7 and 8 f_Q/f_{Q_0} ratios from this study along with f_Q/f_{Q_0} ratios published in the literature are shown. Note that both Gomà and Sterpin (2019) and Gomà *et al* (2016) used the same $W_{\text{air},Q}$ values as in this study.

For the plane-parallel chambers the f_Q/f_{Q_0} ratios between this study and Gomà and Sterpin (2019) agree within two standard uncertainties or better for low energies, except for the IBA PPC-05. For high energies the difference in f_Q/f_{Q_0} ratios increases up to 2.2%. The agreement between this study and Gomà *et al* (2016) is better compared to the agreement with Gomà and Sterpin (2019) except for the IBA PPC-05. However, the chamber model used by Gomà *et al* (2016) is different from that used in this study as discussed by Gomà and Sterpin (2019).

The same can be seen for the cylindrical chambers: while the maximum difference between this study and Gomà and Sterpin (2019) is 1.8% for the NE 2571, the maximum difference between this study and Gomà *et al* (2016) is 0.8%.
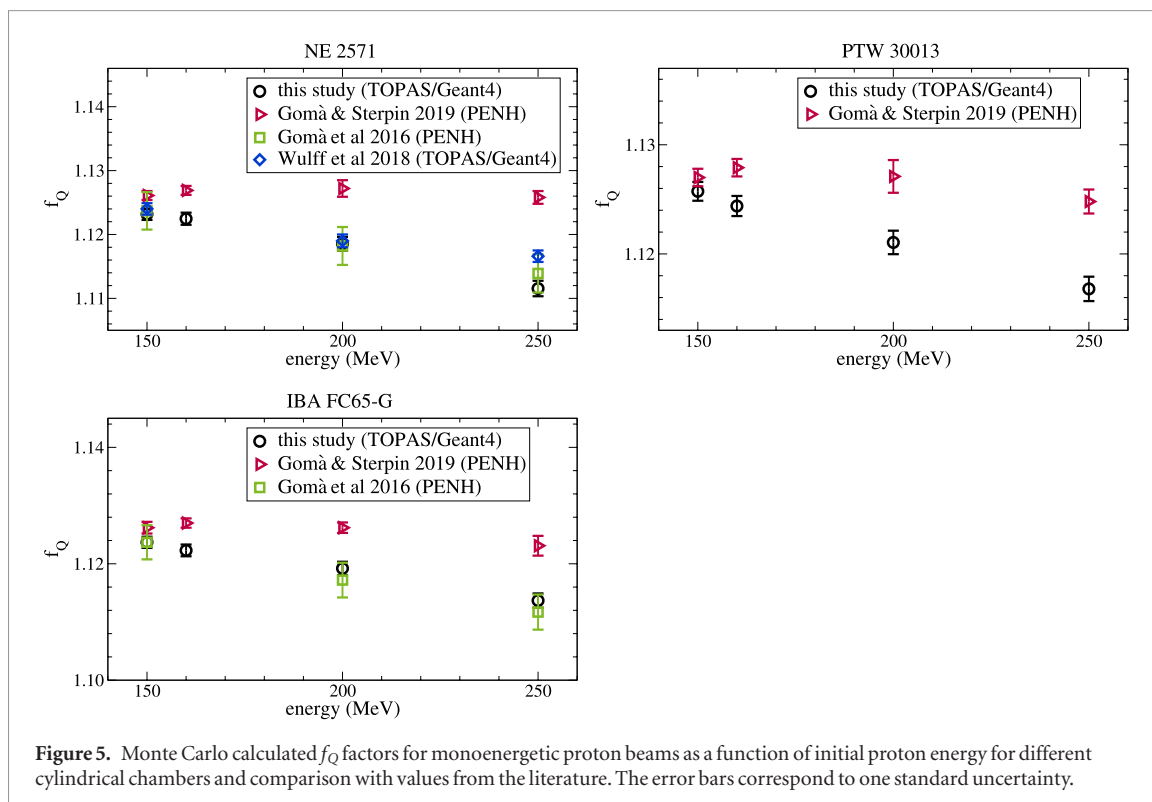
Figure 5. Monte Carlo calculated f_Q factors for monoenergetic proton beams as a function of initial proton energy for different cylindrical chambers and comparison with values from the literature. The error bars correspond to one standard uncertainty.
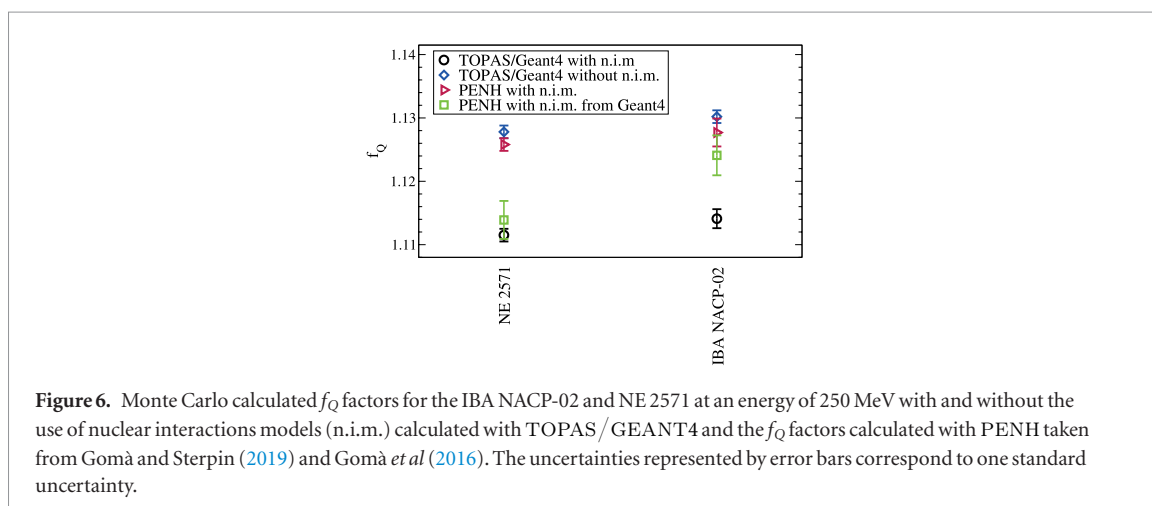

Figure 6. Monte Carlo calculated f_Q factors for the IBA NACP-02 and NE 2571 at an energy of 250 MeV with and without the use of nuclear interactions models (n.i.m.) calculated with $\mathrm{TOPAS}/\mathrm{GEANT4}$ and the f_Q factors calculated with PENH taken from Gomà and Sterpin (2019) and Gomà *et al* (2016). The uncertainties represented by error bars correspond to one standard uncertainty.
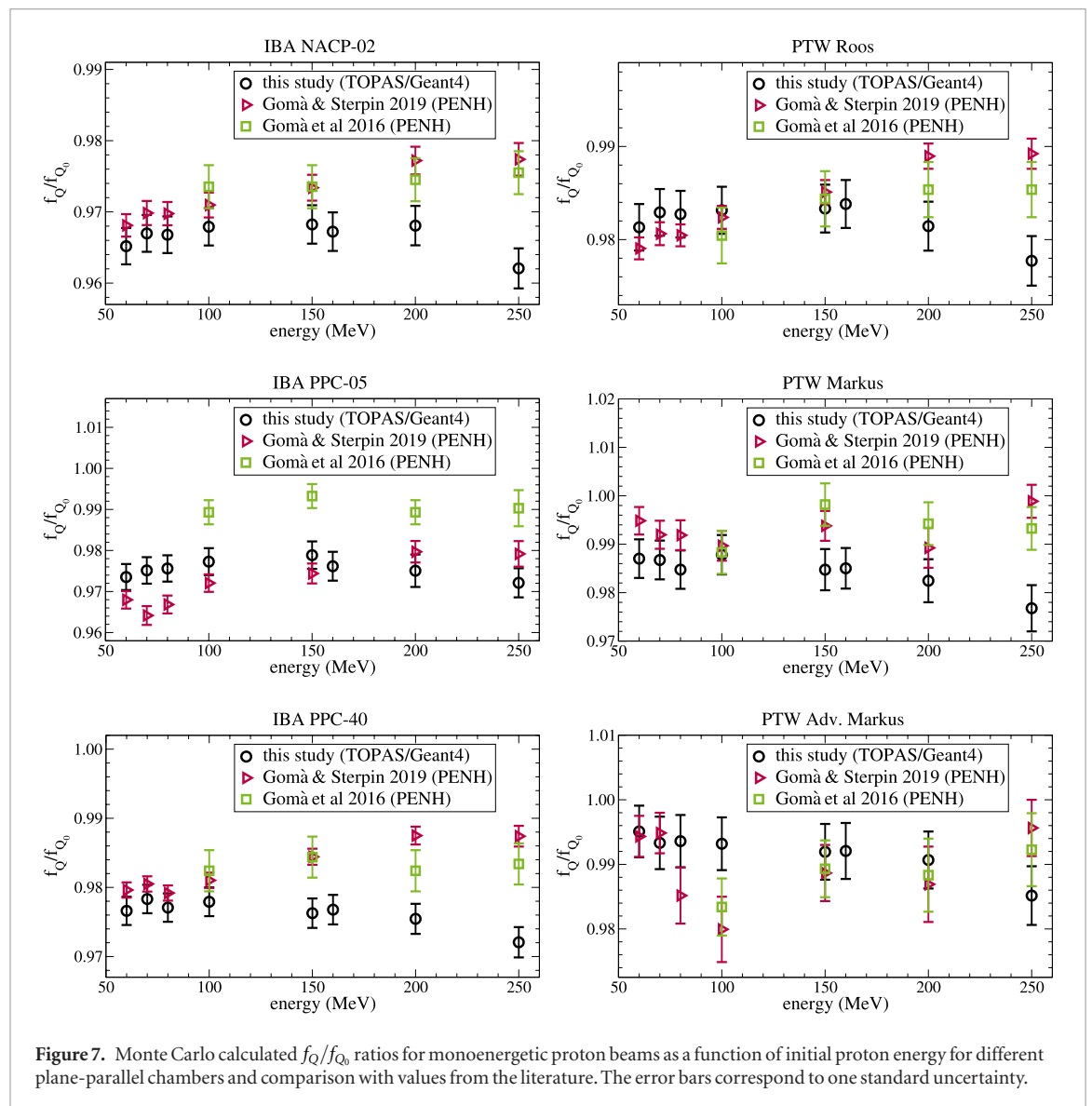
Table 9. Perturbation correction factors for the Exradin A1SL chamber at a proton energy of 250 MeV. The values within parenthesis correspond to one standard uncertainty in the last digit.

Perturbation correction factor	Value
p_{cel}	0.996(4)
p_{stem}	0.995(4)
p_{wall}	0.970(3)
$p_{dis} \cdot p_{cav}$	1.007(3)
p_Q	0.969(7)

In general, the agreement for low energies is better than for higher energies. The differences for high energies might be due to differences in the nuclear interaction models used in the different Monte Carlo codes as discussed above and by Gomà *et al* (2016) and in parts by Baumann *et al* (2019). Of course, the differences in f_Q/f_{Q_0} ratios might also be due to slight differences in the geometry of the chamber models and the materials used between this study and Gomà and Sterpin (2019) and Gomà *et al* (2016). Note that Gomà and Sterpin (2019) provided the physical densities and mean excitation energies of the materials used in their study which are approximately the same values as used in this study, except for small differences in some plastics. Gomà *et al* (2016) did not provide these values. Furthermore, in a study by Baumann *et al* (2019) f_Q/f_{Q_0} ratios were calculated for simple

Table 10. Monte Carlo calculated k_Q factors for monoenergetic proton beams as a function of initial proton energy and the depth z_{ref} at which the chambers were positioned. The values within parenthesis correspond to one standard uncertainty in the last digit.

Q	60 MeV	70 MeV	80 MeV	100 MeV	150 MeV	160 MeV	200 MeV	250 MeV
z_{ref} (g cm^{-2})	1	1	2	2	2	2	2	2
PTW Roos	0.995(6)	0.997(6)	0.996(6)	0.997(6)	0.997(6)	0.997(6)	0.995(6)	0.991(6)
PTW Markus	1.001(7)	1.000(7)	0.998(7)	1.001(7)	0.998(7)	0.999(7)	0.996(7)	0.990(7)
PTW Adv. Markus	1.009(7)	1.007(7)	1.007(7)	1.007(7)	1.006(7)	1.006(7)	1.004(7)	0.999(7)
IBA NACP-02	0.979(6)	0.980(6)	0.980(6)	0.981(6)	0.982(6)	0.981(6)	0.981(6)	0.975(6)
IBA PPC-05	0.987(6)	0.989(6)	0.989(6)	0.991(6)	0.992(6)	0.990(6)	0.989(6)	0.986(6)
IBA PPC-40	0.990(6)	0.992(6)	0.991(6)	0.991(6)	0.990(6)	0.990(6)	0.989(6)	0.986(6)
NE 2571					1.026(6)	1.025(6)	1.022(6)	1.015(6)
PTW 30013					1.027(6)	1.025(6)	1.022(6)	1.018(6)
IBA FC65-G					1.026(6)	1.024(6)	1.022(6)	1.017(6)
Exradin A1SL					1.019(7)	1.015(7)	1.015(7)	1.006(8)

Figure 7. Monte Carlo calculated f_Q/f_{Q_0} ratios for monoenergetic proton beams as a function of initial proton energy for different plane-parallel chambers and comparison with values from the literature. The error bars correspond to one standard uncertainty.

air-filled cavities as representatives of plane-parallel and cylindrical ionization chambers with different Monte Carlo codes (PENH, FLUKA and TOPAS/GEANT4). A monoenergetic 150 MeV proton beam has been used and the cavities were positioned at a depth of 2 g cm^{-2}. The maximum deviation of the f_Q/f_{Q_0} ratios between the codes was 0.7%. The maximum difference of f_Q/f_{Q_0} ratios found in this study for an energy of 150 MeV for the plane-parallel chambers is 1.4%. For the cylindrical chambers and an energy of 150 MeV it is 0.8%. Hence, the
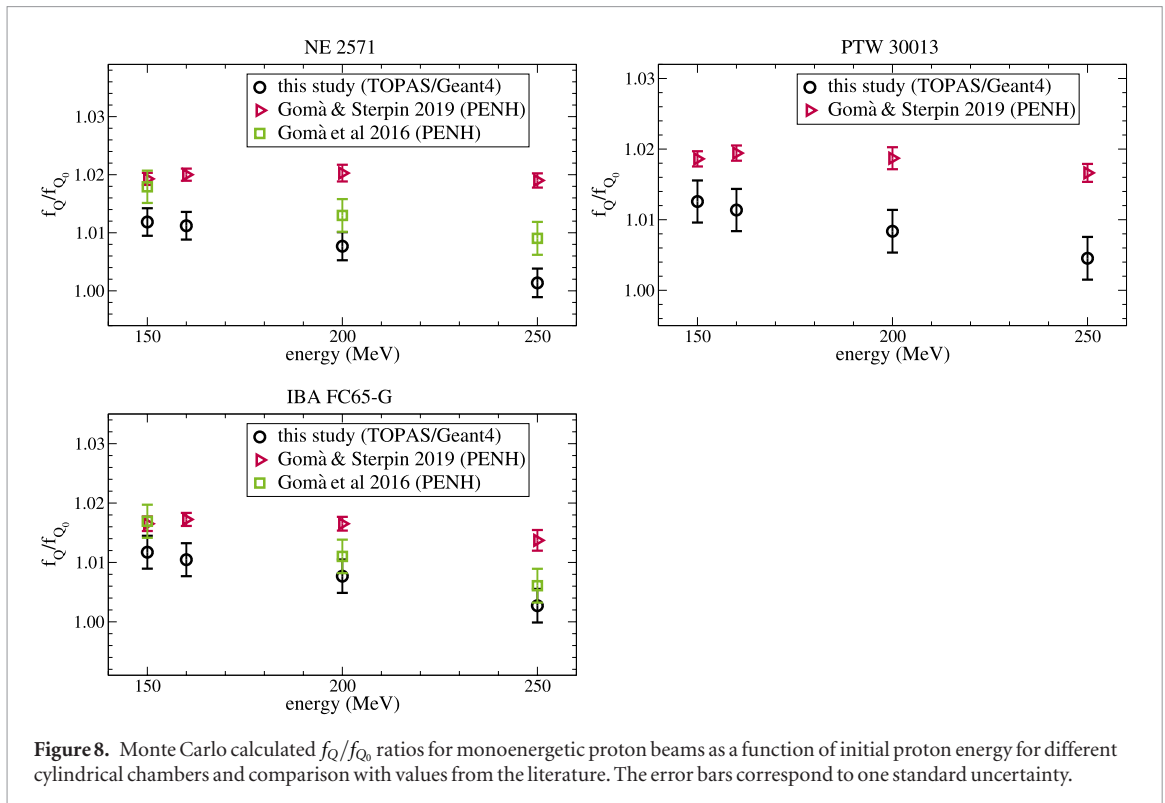
Figure 8. Monte Carlo calculated f_Q/f_{Q_0} ratios for monoenergetic proton beams as a function of initial proton energy for different cylindrical chambers and comparison with values from the literature. The error bars correspond to one standard uncertainty.

Table 11. Ratios of k_Q factors in a 70 MeV monoenergetic proton beam, at a reference depth of $2\,\mathrm{g\,cm^{-2}}$, for different ionization chambers studied in this study and comparison with experimental values in the literature for non-modulated beams. The values within parenthesis correspond to one standard uncertainty in the last digit. In the right column the relative deviations between the values from this study and the values from the literature are given.

Ionization chambers	This study	Palmans *et al* (2001)	Palmans *et al* (2002)	Deviation (%)
IBA FC65-G/NE 2571	1.000(4)	0.997(3)		0.3
IBA NACP-02/NE 2571	0.920(3)		0.930(3)	−1.0
PTW Markus/NE 2571	0.942(4)		0.940(3)	0.2
PTW Roos/NE 2571	0.935(2)		0.937(3)	−0.2
R_{res} ($\mathrm{g\,cm^{-2}}$)	2.10	2.65	2.65	

deviations of f_Q/f_{Q_0} ratios for real ionization chambers are in the order of the deviations for simple air-filled cavities, although the geometries are more complex.

To validate whether the nuclear interaction models lead to larger deviations between the Monte Carlo codes independent on the chamber geometry, we re-calculated the simulations for simple air-filled cavities as done by Baumann *et al* (2019) for an energy of 250 MeV. We used exactly the same geometries, physics lists and source parameters. The largest difference between $\mathrm{TOPAS/GEANT4}$ and PENH for an energy of 250 MeV was 0.6% and hence comparable to the differences observed for an energy of 150 MeV. Interestingly, the difference between the codes does not increase with energy for simple air-filled cavities as it is the case for the ionization chambers. Hence, it might be that differences between the codes occur because of the materials and/or complexity of the chamber geometries.

In order to further validate the k_Q factors calculated with $\mathrm{TOPAS/GEANT4}$ in this study, in table 11 the ratios of k_Q factors are shown for some of the ionization chambers and compared to experimental data. Palmans *et al* (2001) and Palmans *et al* (2002) determined experimentally the ratios of k_Q factors between different chambers and the NE 2571 as a reference chamber. A non-modulated proton beam with $R_{\mathrm{res}} = 2.65$ cm has been used. Hence, we re-calculated the corresponding chambers (NE 2571, IBA FC65-G, IBA NACP-02, PTW Markus and PTW Adv. Markus) in a 70 MeV monoenergetic proton beam ($R_{\mathrm{res}} = 4.10$ cm) at a depth of $2\,\mathrm{g\,cm^{-2}}$. In the studies by Palmans *et al* (2001) and Palmans *et al* (2002) the ratios of k_Q factors were not reported explicitly but can be found in Gomà *et al* (2016). For all four ratios of k_Q factors the deviation between the ratios calculated in this study and the experimentally determined values are 1% at maximum.

In table 12 ratios of k_Q factors are shown for several ionization chambers that were determined by Gomà *et al* (2015). For the comparison we took the values determined in a non-modulated proton beam with $R_{\mathrm{res}} \approx 6$ cm. This corresponds to an initial proton energy of 100 MeV and a chamber depth of $2\,\mathrm{g\,cm^{-2}}$. Hence, we calculated the k_Q factors for the IBA FC65-G and PTW 30013 in a 100 MeV proton beam at that depth. For the IBA NACP-02,

Table 12. Ratios of k_Q factors in a 100 MeV monoenergetic proton beam, at a reference depth of $2 \, \mathrm{g \, cm^{-2}}$, for different ionization chambers studied in this study and comparison with experimental values in the literature for non-modulated beams. The values within parenthesis correspond to one standard uncertainty in the last digit. In the right column the relative deviations between the values from this study and the values from the literature are given.

Ionization chambers	This study	Gomà *et al* (2015)	Deviation (%)
IBA NACP-02/FC65-G	0.947(4)	0.943(4)	0.4
PTW Adv. Markus/FC65-G	0.972(5)	0.949(4)	2.4
PTW Markus/FC65-G	0.967(5)	0.953(4)	1.4
PTW Roos/FC65-G	0.962(4)	0.960(4)	0.2
PTW 30013/FC65-G	0.999(4)	1.002(4)	−0.3
R_{res} ($\mathrm{g \, cm^{-2}}$)	5.76	5.93	

Table 13. Monte Carlo calculated k_Q factors in monoenergetic proton beams for different ionization chambers studied in this study and comparison with experimental values in the literature for non-modulated beams. The values within parenthesis correspond to one standard uncertainty in the last digit(s). In the right column the relative deviations between the values from this study and the values from the literature are given.

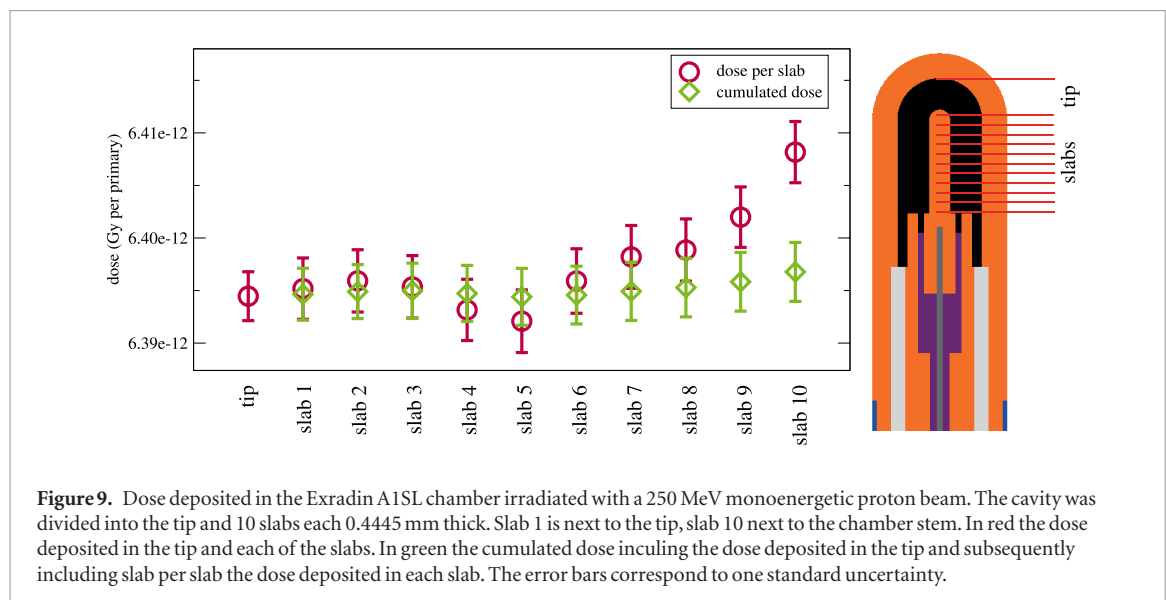| Ionization chamber	Energy (MeV)	This study	Medin *et al* (2006)	Medin (2010)	Deviation (%)
IBA FC65-G	150	1.026(6)	1.021(7)		0.5
NE 2571	150	1.026(6)	1.021(7)		0.5
NE 2571	160	1.025(6)		1.032(13)	−0.7

PTW Roos and PTW 30013 the deviations of the ratios of k_Q factors calculated in this study are smaller than 0.5% compared to the experimentally determined ratios. For the PTW Markus chamber the deviation is 1.4% and for the PTW Adv. Markus it is 2.4%. Note that the deviation for the ratio of k_Q factors including the PTW Markus chamber is only 0.2% compared to the experimentally determined ratio of k_Q factors from Palmans *et al* (2002) (see table 11).

At last, Medin (2010) experimentally determined the k_Q factor for the NE 2571 in a proton beam with $R_{res} = 16.5 \, \mathrm{cm}$. Correspondingly, we took the k_Q factor calculated for an initial energy of 160 MeV at a depth of $2 \, \mathrm{g \, cm^{-2}}$ ($R_{res} = 15.74 \, \mathrm{g \, cm^{-2}}$). Medin *et al* (2006) experimentally determined the k_Q factors for the NE 2571 and the IBA FC65-G and a proton beam with $R_{res} = 14.7 \, \mathrm{cm}$. Correspondingly, we took the k_Q factors calculated for an initial energy of 150 MeV at a depth of $2 \, \mathrm{g \, cm^{-2}}$ ($R_{res} = 13.85 \, \mathrm{g \, cm^{-2}}$). The k_Q factors calculated in this study as well as the experimentally determined values by Medin (2010) and Medin *et al* (2006) are shown in table 13. The maximum deviation between the k_Q factors calculated in this study relative to the k_Q factors determined experimentally is 0.7%.

In conclusion, the comparison of k_Q factors and ratios of k_Q factors calculated in this study using the Monte Carlo code TOPAS/GEANT4 with experimental values shows good agreement on the 1% level with only two exceptions for the PTW Adv. Markus chamber (2.4%) and the PTW Markus chamber (1.4%). However, for the PTW Markus chamber we also found good agreement (deviation of only 0.2%) when the ratio of k_Q factors was compared to the experimentally determined values from Palmans *et al* (2002).

3.5. Possible influence of the death volume for ionization chambers

In figure 9 the dose deposited in the Exradin A1SL chamber irradiated with a 250 MeV monoenergetic proton beam is shown. The cavity was divided into the tip and 10 slabs each 0.4445 mm thick. Slab 1 is next to the tip, slab 10 next to the chamber stem. In red the dose deposited in the tip and each of the slabs. In green the cumulated dose: the cumulated dose for slab *i* averages the doses deposited in the tip and in the slabs 1 to *i*. It can be seen that the dose deposited in the different slabs varies by up to 0.25% at maximum while the dose increases towards the chamber stem. The larger dose deposited in the slabs in the vicinity of the chamber stem might be due to secondary particles (e.g. electrons) produced in the stem that are being scattered into the cavity. However, due to the short range of these secondary particles, the influence on the dose in the complete cavity is small which is in agreement with the finding that the perturbation correction factor for the chamber stem is 0.995(3) and hence roughly 1. The cumulated dose is quasi-constant over the complete cavity while the maximum deviation between any two cumulated dose values is 0.04%, which is not significant (one standard deviation is ∼0.05% for each cumulated dose value). Following the study by Pojtinger *et al* (2019), the death volume is located in the vicinity of the guard ring and hence the chamber stem. Since the cumulated dose is quasi-constant over the complete cavity, it does not matter how large the sensitive volume is: for example, if the sensitive volume is restricted to the tip, the dose measured with the chamber would not be significantly different from the dose measured if the sensitive volume was consisting of the tip and any number of slabs. Hence, the influence of the death volume on the dose deposited in the cavity is negligible for this investigated chamber and does not influence the calculation of k_Q factors significantly. Since the other cylindrical

Figure 9. Dose deposited in the Exradin A1SL chamber irradiated with a 250 MeV monoenergetic proton beam. The cavity was divided into the tip and 10 slabs each 0.4445 mm thick. Slab 1 is next to the tip, slab 10 next to the chamber stem. In red the dose deposited in the tip and each of the slabs. In green the cumulated dose inculing the dose deposited in the tip and subsequently including slab per slab the dose deposited in each slab. The error bars correspond to one standard uncertainty.

ionization chambers investigated in this study have a larger cavity compared to the Exradin A1SL, the results from this investigation should be applicable to the other cylindrical chambers, as well.

4. Conclusion

The Monte Carlo code $\mathrm{TOPAS}/\mathrm{GEANT4}$ was used to calculate f_{Q_0} factors in a ^{60}Co spectrum and f_Q factors in monoenergetic proton beams for six plane-parallel and four cylindrical ionization chambers. From these factors k_Q factors were derived. The comparison of k_Q factors calculated in this study with experimentally determined k_Q factors and ratios of k_Q factors showed good agreement on the 1% level. Hence, $\mathrm{TOPAS}/\mathrm{GEANT4}$ can be used to calculate k_Q factors for ionization chambers in monoenergetic proton beams. The comparison with other Monte Carlo calculated f_Q/f_{Q_0} ratios showed that the role of nuclear interaction models has to be investigated further for high proton energies.

Additionally, perturbation correction factors for the Exradin A1SL chamber in a 250 MeV monoenergetic proton beam were calculated. It can be concluded that the assumption of the IAEA TRS-398 CoP (that all perturbation correction factors in proton beams are 1 for all ionization chambers) might not be sufficiently accurate for all chambers and proton energies—especially in the case for the factor p_{wall}.

Acknowledgments

ORCID iDs

Kilian-Simon Baumann ⓘ https://orcid.org/0000-0003-1223-523X
Klemens Zink ⓘ https://orcid.org/0000-0001-5785-4101

References

Agostinelli S *et al* 2003 Geant4—a simulation toolkit *Nucl. Instrum. Methods Phys. Res.* A **506** 250–303
Andreo P *et al* 2019 Determinatin of consensus k_Q mean values for megavoltage photon beams for the update of IAEA TRS-398 *Phys. Med. Biol.* (submitted)
Andreo P, Burns D T, Hohlfeld K, Huq M S, Kanai T, Laitano F, Smyth V and Vynicker S 2000 Absorbed dose determination in external beam radiotherapy: an international code of practice for dosimetry based on standards of absorbed dose to water *Technical Report* Technical Report Series TRS-398 (Vienna: International Atomic Energy Agency) (http://www-naweb.iaea.org/nahu/DMRP/documents/ CoP_V12_2006-06-05.pdf)

Andreo P, Wulff J, Burns D T and Palmans H 2013 Consistency in reference radiotherapy dosimetry: resolution of an apparent conundrum when ^{60}Co is the reference quality for charged-particle and photon beams *Phys. Med. Biol.* **58** 6593–621

Arce P *et al* 2014 Gamos: a framework to do GEANT4 simulations in different physics fields with an user-friendly interface *Nucl. Instrum. Methods Phys. Res.* A **735** 304–13

Barschall H H, Chadwick M B, Jones D L T, Meulders J P, Schuhmacher H and Young P G 2000 Nuclear data for neutron and proton radiotherapy and for radiation protection *ICRU Report* 63 International Commission on Radiation Units and Measurements (https://inis.iaea.org/collection/NCLCollectionStore/_Public/32/048/32048887.pdf)

Baumann K S, Horst F, Zink K and Gomà C 2019 Comparison of PENH, FLUKA, and GEANT4/TOPAS for absorbed dose calculations in air cavities representing ionization chambers in high-energy photon and proton beams *Med. Phys.* **46** 4639–53

Bielajew A 2016 Fundamentals of the Monte Carlo method for neutral and charged particle transport The University of Michigan, Department of Nuclear Engineering and Radiological Sciences (http://www.umich.edu/~nersb590/CourseLibrary/MCbook.pdf)

Böhlen T T, Cerutti F, Chin M P W, Fassò A, Ferrari A, Ortega P G, Mairani A, Sala P R, Smirnov D and Vlachoudis V 2014 The FLUKA code: developments and challenges for high energy and medical applications *Nucl. Data Sheets* **120** 211–4

Czarnecki D, Poppe B and Zink K 2018 Impact of new ICRU report 90 recommendations on calculated correction factors for reference dosimetry *Phys. Med. Biol.* **63** 155015

Erazo F, Brualla L and Lallena A M 2014 Electron beam quality k_Q, q0 factors for various ionization chambers: a Monte Carlo investigation with penelope *Phys. Med. Biol.* **59** 6673–91

Ferrari A, Sala P R, Fasso A and Ranft J 2005 FLUKA: a multi-particle transport code *Technical Report* CERN-2005-10, INFN/TC 05/11, SLAC R-773 (Geneva: CERN) (https://doi.org/10.2172/877507)

Folger G, Ivanchenko V N and Wellisch J P 2004 The binary cascade *Eur. Phys. J.* A **21** 407–17

Gomà C and Sterpin E 2019 Monte Carlo calculation of beam quality correction factors in proton beams using PENH *Phys. Med. Biol.* **64** 185009

Gomà C, Andreo P and Sempau J 2016 Monte Carlo calculation of beam quality correction factors in proton beams using detailed simulation of ionization chambers *Phys. Med. Biol.* **61** 2389–406

Gomà C, Hofstetter-Boillat B, Safai S and Vörös S 2015 Experimental validation of beam quality correction factors for proton beams *Phys. Med. Biol.* **60** 3207–16

Goudsmit S and Saunderson J L 1940a Multiple scattering of electrons *Phys. Rev.* **57** 552

Goudsmit S and Saunderson J L 1940b Multiple scattering of electrons II *Phys. Rev.* **58** 36

Ivanchenko V N, Kadri O, Maire M and Urban L 2010 Geant4 models for simulation of multiple scattering *J. Phys.: Conf. Ser.* **219** 032045

Lourenço A, Bouchard H, Galer S, Royle G and Palmans H 2019 The influence of nuclear interactions on ionization chamber perturbation factors in proton beams: FLUKA simulations supported by a Fano test *Med. Phys.* **46** 885–91

Mainegra-Hing E and Muir B R 2018 On the impact of ICRU report 90 recommendations on kQ factors for high-energy photon beams *Med. Phys.* **45** 3904–8

Medin J 2010 Implementation of water calorimetry in a 180 MeV scanned pulsed proton beam including an experimental determination of kQ for a farmer chamber *Phys. Med. Biol.* **55** 3287–98

Medin J, Ross C K, Klassen N V, Palmans H, Grusell E and Grindborg J E 2006 Experimental determination of beam quality factors, kQ, for two types of farmer chamber in a 10 MV photon and a 175 MeV proton beam *Phys. Med. Biol.* **51** 1503–21

Mora G M, Maio A and Rogers D W O 1999 Monte carlo simulation of a typical Co-60 therapy source *Med. Phys.* **26** 2494–502

Muir B R and Rogers D W O 2010 Monte Carlo calculations of, the beam quality conversion factor *Med. Phys.* **37** 5939–50

Muir B R, McEwen M R and Rogers D W O 2012 Beam quality conversion factors for parallel-plate ionization chambers in MV photon beams *Med. Phys.* **39** 1618–31

O'Brien D J, Roberts D A, Ibbot G S and Sawakuchi G O 2016 Reference dosimetry in magnetic fileds: formalism and ionization chamber correction factors *Med. Phys.* **43** 4915–27

Palmans H, Verhaegen F, Denis J M and Vynckier S 2002 Dosimetry using plane-parallel ionization chambers in a 75 MeV clinical proton beam *Phys. Med. Biol.* **47** 2895–905

Palmans H, Verhaegen F, Denis J M, Vynckier S and Thierens H 2001 Experimental p_{wall} and p_{cel} correction factors for ionization chambers in low-energy clinical proton beams *Phys. Med. Biol.* **46** 1187–204

Panettieri V, Sempau J and Andreo P 2008 Chamber-quality factors in60co for three plane-parallel chambers for the dosimetry of electrons, protons and heavier charged particles: PENELOPE Monte Carlo simulations *Phys. Med. Biol.* **53** 5917–26

Perl J, Shin J, Schuemann J, Faddegon B and Paganetti H 2012 TOPAS: an innovative proton Monte Carlo platform for research and clinical applications *Med. Phys.* **39** 6818–37

Pojtinger S, Kapsch R P, Dohm O S and Thorwarth D 2019 A finite element method for the determination of the relative response of ionization chambers in MR-linacs: simulation and experimental validation up to 1.5 T *Phys. Med. Biol.* **64** 135011

RTNORM 2019 Radiotherapy normative, 'ionizing radiation dosimetry for radiotherapy', euramet/empir research project (2017–2019) (Accessed: 5 February 2020) (www.rtnorm.eu)

Salvat F 2013 A generic algorithm for Monte Carlo simulation of proton transport *Nucl. Instrum. Methods Phys. Res.* B **316** 144–59

Seltzer S M, Fernández-Verea J M, Andreo P, Bergstrom P M, Burns D T, Krajcar Bronić I, Ross C K and Salvat F 2016 Key data for ionizing-radiation dosimetry: measurement standards and applications. ICRU Report 90 *J. ICRU* **14** 1–110

Sempau J and Andreo P 2006 Configuration of the electron transport algorithm of penelope to simulate ion chambers *Phys. Med. Biol.* **51** 3533–48

Sempau J, Andreo P, Aldana J, Mazurier J and Salvat F 2004 Electron beam quality correction factors for plane-parallel ionization chambers: Monte Carlo calculations using the PENELOPE system *Phys. Med. Biol.* **49** 4427–44

Simiele E and DeWerd L 2018 On the accuracy and efficiency of condensed history transport in magnetic fields in GEANT4 *Phys. Med. Biol.* **63** 235012

Testa M, Schuemann J, Lu H M, Shin J, Faddegon B, Perl J and Paganetti H 2013 Experimental validation of the TOPAS Monte Carlo system for passive scattering proton therapy *Med. Phys.* **40** 121719

Urban L 2002 Multiple scattering model in GEANT4 *Report No. CERN-OPEN-2002-070* (Geneva: CERN) (https://cds.cern.ch/record/592633)

Wulff J, Baumann K S, Verbeek N, Bäumer C, Timmermann B and Zink K 2018 TOPAS/GEANT4 configuration for ionization chamber calculations in proton beams *Phys. Med. Biol.* **63** 115013

Wulff J, Heverhagen J T and Zink K 2008 Monte-Carlo-based perturbation and beam quality correction factors for thimble ionization chambers in high-energy photon beams *Phys. Med. Biol.* **53** 2823–36

Zink K and Wulff J 2012 Beam quality corrections for parallel-plate ion chambers in electron reference dosimetry *Phys. Med. Biol.* **57** 1831–54